Proceedings of the 17th World Congress
The International Federation of Automatic Control
Seoul, Korea, July 6-11, 2008

Senseless Maneuver Optimal Washout Filter Design with Human Vestibular Based (HVB) for VR-based Motion Simulator

Chin-I Huang [1] *** and Li-Chen, Fu** [2]

[1] *Department of Automation Engineering, National Formosa University,*

[2] *Department of Electrical Engineering, National Taiwan University*
(e-mail: chini@ieee.org, lichen@ntu.edu.tw)

Abstract: In this paper, we propose a new approach "HVB senseless maneuver optimal washout filter" which is based on human vestibular system, senseless maneuver and motion platform limitation for designing washout filter such that a cost function constraining the pilot sensation error (between simulator and vehicle) is minimized. This approach can curtail over strong feelings of pilot reception and increase efficiency of platform workspace for task running. Finally, the experimental results confirm the effectiveness of our algorithm hereby proposed. Moreover, the results show that a better performance can be attained.

1. INTRODUCTION

The washout filter, whose name originates from the fact that one of its functions is to "wash out" the position of the simulator back to its neutral point, remain the dominant source of poor fidelity in the motion cues, and even a small refinement in this area can yield a significant improvement in motion realism [1].

Many different schemes of washout filter have been proposed in the last three decades [2]. Classical washout filter [1,6] was the first kind that has been developed, which is composed of linear low-pass filters and high-pass filters and is featured by its simplicity and ease of adjustment. But owing to the inflexibility of the classical washout filter, many washout algorithms with the parameter self-tuning mechanism have been proposed to solve this problem. The adaptive scheme tunes the filter gain in real time to minimize a cost function using steepest descent techniques [1]. Recently, an auto-tuning washout filter based on the adaptive algorithm and neuro-fuzzy network is proposed [3]. Besides, considering the situation where the motion platform may be subjected to limited bandwidth, low driven power, or poor position control, a robust control algorithm which adopts the closed-loop form with feedback of the platform position, attitude, and even accelerometer measurement is proposed [4,8].

The optimal control algorithm is characterized by a systematic combination of linear filters that are determined through an off-line design process which produces the optimal form, order, and characteristics of the filters given the underlying assumptions [7]. However, there has been no consideration of "tilt-rate limiting", in the design of washout filters, and this has imposed adverse effects on fidelity of the pilot perception. To solve this problem, the senseless maneuver is proposed in our approach, and the mechanical limitation of the motion platform is also considered to increase the efficiency of the platform workspace usage for running various tasks.

This paper is organized as follows. Tthe human senseless maneuver is proposed in section 2. Then, the human vestibular based (HVB) optimal washout filter is proposed in section 3. After that, experiment results are provided to confirm the effectiveness of the developed result in section 4. Finally, the conclusion is made in section 5.

3. HUMAN SENSLESS MANEUVER DESIGN

The main idea of this algorithm is to directly manage the trajectory of motion platform under the premise of not interfering the original perception of the operator. To make the movement "senseless" to the operator, the acceleration must be under the threshold value of human perception (Table 1).

Table 1. Sensation Threshold Value of Otolith [5]

	Surge	Sway	Heave
$d_m(m/\sec^2)$	0.17	0.17	0.28

If we move the platform only in translational directions, the induced acceleration on body-axis and inertial-axis will be exactly the same. Such motion will be slow and inefficient under the constraint of being "senseless".

We propose a new method which treats the operator as an inverted pendulum. The control goal of the inverted pendulum is to move the pendulum with attitude change as small as possible.

For the inverted pendulum, the linkage between car and pendulum is ball joint. Actually, there isn't any joint between operator and his seat. However, if the platform tilts the same angle as that of the pendulum, the stability problem will be the same as that shown in Fig. 1.

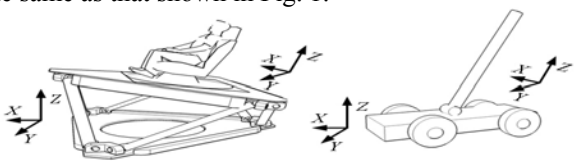

Fig.1 Schematics of Senseless Maneuver

This algorithm itself is not a complete washout filter. It is a function which provides a method to move the platform directly and senselessly. In other words, by a simple superposition of the output signal of this method and that of washout filter, the performance can be improved by a better usage of the platform workspace. Fig. 2 is a schematic of the combination of senseless maneuver and human vestibular system based optimal washout filter. About how to design human vestibular system based optimal washout filter is shown next section.

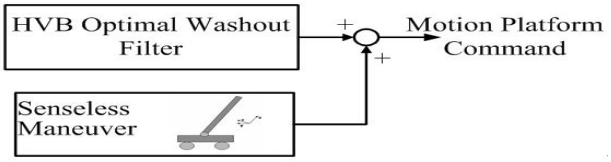

Fig.2 Schematics of HVB Optimal Washout Filter with Senseless Maneuver

4. HUMAN VESTIBULAR BASED OPTIMAL WASHOUT FILTER DESIGN

In developing a washout filter, the problem is to determine a transfer function matrix *W(s)* that relates the desired simulator's motion input to the vehicle's input such that a cost function constraining the pilot sensation error (between the simulator and the vehicle) is minimized. The structure of this problem is illustrated in Fig. 3.

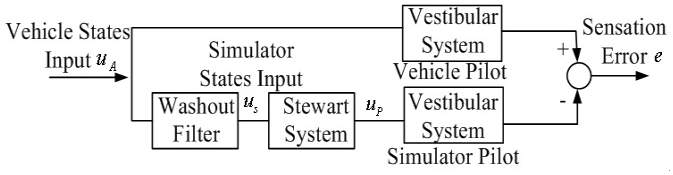

Fig. 3 Underlying Problem Structure

4.1 Longitudinal Mode

The algorithm under development with angular velocity input for the longitudinal (pitch/surge) mode is described below. The input u is formulated as

$$u = \begin{bmatrix} \dot{\theta} \\ a_x \end{bmatrix} \tag{1}$$

where $\dot{\theta}$ is angular velocity and a_x is the translational acceleration, referring to Fig. 6.

The sensed angular motion $\dot{\hat{\theta}}$ is related to $\dot{\theta}$ by the semicircular canals model [5] as:

$$\dot{\hat{\theta}} = \frac{G_{sc}\tau_1\tau_a s^2(1+\tau_L s)}{(1+\tau_a s)(1+\tau_1 s)(1+\tau_2 s)}\dot{\theta} \tag{2}$$

where the semicircular canals time constants are τ_1, τ_2, τ_a and τ_L, and G_{sc} is the angular velocity threshold that scales the response to threshold units. For realization purpose, Eq. (2) can be rewritten as

$$\dot{\hat{\theta}} = \frac{T_4 s^3 + T_3 s^2}{s^3 + T_2 s^2 + T_1 s + T_0}\dot{\theta} \tag{3}$$

where

$$T_0 = \frac{1}{\tau_a\tau_1\tau_2}, T_1 = \frac{\tau_a+\tau_1+\tau_2}{\tau_a\tau_1\tau_2}, T_1 = \frac{\tau_1\tau_2+\tau_a(\tau_1+\tau_2)}{\tau_a\tau_1\tau_2}, T_3 = \frac{G_{sc}}{\tau_2}$$
$$, T_4 = \frac{G_{sc}\tau_L}{\tau_2},$$

and can be defined in state space notation as

$$\dot{X}_{sc} = A_{sc}X_{sc} + B_{sc}u$$
$$\dot{\hat{\theta}} = C_{sc}X_{sc} + D_{sc}u \tag{4}$$

with the parameter setting chosen in observer canonical form as :

$$A_{sc} = \begin{bmatrix} -T_2 & 1 & 0 \\ -T_1 & 0 & 1 \\ -T_0 & 0 & 0 \end{bmatrix}, B_{sc} = \begin{bmatrix} T_3 - T_2T_4 & 0 \\ -T_1T_4 & 0 \\ -T_0T_4 & 0 \end{bmatrix}, C_{sc} = \begin{bmatrix} 1 & 0 & 0 \end{bmatrix} \text{ and}$$
$$D_{sc} = \begin{bmatrix} T_4 & 0 \end{bmatrix}.$$

The sensed specific force $\hat{f}_x$ is related to the stimulus specific force f_x by the otolith model [5]

$$\hat{f}_x = \frac{G_{ot}K_{ot}(s+a_0)}{(s+b_0)(s+b_1)}f_x \tag{5}$$

where a_0, b_0, b_1 and K_{ot} are computed parameters of the otolith model, and G_{ot} is the linear acceleration threshold that scales the response to threshold units.

For the centre of rotation at the centroid of the motion platform, the specific force is

$$f_x = a_x + g\theta - r_{cp}\ddot{\theta} \tag{6}$$

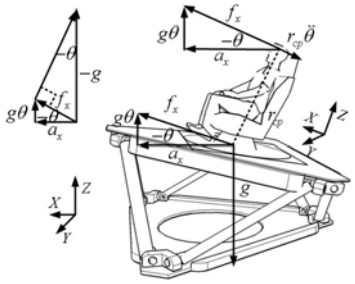

Fig.4 Inertial and Body Coordinate of Motion Platform

where r_{cp} is the radius from the centroid of the motion platform to the pilot's head. Then, transform Eq. (6) into its Laplace form, and we obtain

$$f_x(s) = a_x(s) + (g\frac{1}{s} - r_{cp}s)\dot{\theta}(s), \tag{7}$$

which is substituted into (5) to result in

$$\hat{f}_x = \frac{G_{ot}K_{ot}(s+a_0)}{(s+b_0)(s+b_1)}(a_x(s) + (g\frac{1}{s} - r_{cp}s)\dot{\theta}(s))$$
$$= G_{ot}K_{ot}\begin{bmatrix} \frac{-r_{cp}s^3 - r_{cp}s^2 + gs + ga_0}{s(s+b_0)(s+b_1)} & \frac{s+a_0}{(s+b_0)(s+b_1)} \end{bmatrix}u \tag{8}$$

Rearranging and taking derivatives of Eq. (8) leads to the following differential equation

$$\dddot{\hat{f}}_x + (b_0+b_1)\ddot{\hat{f}}_x + b_0b_1\dot{\hat{f}}_x$$
$$= G_{ot}K_{ot}(r_{cp}(b_0+b_1-a_0)\ddot{\theta}$$
$$+(g + r_{cp}b_0b_1)\theta + ga_0\int\theta dt + \dot{a}_x + a_0a_x) \tag{9}$$

which can be rewritten as

$$\dddot{\hat{f}}_x + a\ddot{\hat{f}}_x + b\dot{\hat{f}}_x = c\dot{\theta} + d\theta + e\int \theta dt + f\dddot{a}_x + g\ddot{a}_x \quad (10)$$

and can then be defined in state space notation as

$$\dot{X}_{ot} = A_{ot}X_{ot} + B_{ot}u$$
$$\dot{\hat{f}}_x = C_{ot}X_{ot} + D_{ot}u \quad (11)$$

where X_{ot} is the otoliths state vector, and

$$A_{ot} = \begin{bmatrix} 0 & 1 & 0 & 0 & 0 \\ -b & -a & 1 & 0 & 0 \\ 0 & 0 & 0 & 0 & 0 \\ 0 & 0 & 0 & 0 & 1 \\ 0 & 0 & 0 & -b & -a \end{bmatrix}, B_{ot} = \begin{bmatrix} c & 0 \\ d-ac & 0 \\ e & 0 \\ 0 & f \\ 0 & h-af \end{bmatrix},$$
$$C_{ot} = \begin{bmatrix} 1 & 0 & 0 & 1 & 0 \end{bmatrix}, D_{ot} = \begin{bmatrix} -G_{ot}K_{ot}r_{cp} & 0 \end{bmatrix}.$$

The representations in Eqs. (4) and (11) can be integrated to form a single representation for the human vestibular model:

$$\dot{X}_v = A_v X_v + B_v u$$
$$\hat{y}_v = C_v X_v + D_v u \quad (12)$$

where $\dot{X}_v$ and $\hat{y}$ are, respectively, the combined states and sensed responses, and A_v , B_v , C_v and D_v represent the vestibular models as one set of state equations:

$$A_v = \begin{bmatrix} A_{sc} & 0 \\ 0 & A_{ot} \end{bmatrix}, B_v = \begin{bmatrix} B_{sc} \\ B_{ot} \end{bmatrix},$$
$$C_v = \begin{bmatrix} C_{sc} & 0 \\ 0 & C_{ot} \end{bmatrix}, D_v = \begin{bmatrix} D_{sc} \\ D_{ot} \end{bmatrix}.$$

It is assumed that the same sensation model can be applied to both the pilot in the vehicle and the pilot in the simulator as shown in Fig. 4. We then define the vestibular state error $X_e = X_s - X_a$ (where X_s and X_A are the respective vestibular states for the simulator and the vehicle), and the pilot sensation error e, resulting in

$$\dot{X}_e = A_v X_e + B_v u_s - B_v u_A$$
$$e = C_v X_e + D_v u_s - D_v u_A \quad (13)$$

where u_s and u_A represent the simulator inputs and vehicle inputs, respectively, as given in (1).

In order to constrain the simulator motion, it is necessary for the control algorithm to explicitly access states such as the linear velocity and displacement of the simulator that will appear in the cost function. For this purpose, additional terms are included in the state equations:

$$\dot{X}_c = A_c X_c + B_c u_s \quad (14)$$

where X_c represents the additional simulator states:

$$X_c = \begin{bmatrix} \iiint a_x dt^3 & \iint a_x dt^2 & \int a_x dt & \theta \end{bmatrix}^T,$$

u_s is the simulator input, and A_c, B_c are

$$A_c = \begin{bmatrix} 0 & 1 & 0 & 0 \\ 0 & 0 & 1 & 0 \\ 0 & 0 & 0 & 0 \\ 0 & 0 & 0 & 0 \end{bmatrix}, B_c = \begin{bmatrix} 0 & 0 \\ 0 & 0 \\ 0 & 1 \\ 1 & 0 \end{bmatrix}$$

The vehicle input u_A consists of filtered white noise, and can be expressed as

$$\dot{X}_n = A_n X_n + B_n w$$
$$u_A = X_n \quad (15)$$

where X_n is the filtered white noise state vector, w is the white noise, with A_n and B_n being given as

$$A_n = \begin{bmatrix} -\gamma_1 & 0 \\ 0 & -\gamma_2 \end{bmatrix}, B_n = \begin{bmatrix} \gamma_1 \\ \gamma_2 \end{bmatrix}$$

where γ_1 and γ_2 are the first-order filter break frequencies for respective degree-of-freedoms. The state equations described by Eqs. (13), (14), and (15) can be combined to form the desired system equation

$$\dot{X} = AX + Bu_s + Hw$$
$$y = CX + Du_s \quad (16)$$

where $X = \begin{bmatrix} X_e & X_c & X_n \end{bmatrix}^T$ represents the integrated states, $y = \begin{bmatrix} e & X_c \end{bmatrix}^T$ is the desired output, and the combined system matrices A , B , C , D and H are then given by

$$A = \begin{bmatrix} A_v & 0 & -B_v \\ 0 & A_c & 0 \\ 0 & 0 & A_n \end{bmatrix}, B = \begin{bmatrix} B_v \\ B_c \\ 0 \end{bmatrix}, H = \begin{bmatrix} 0 \\ 0 \\ B_n \end{bmatrix},$$
$$C = \begin{bmatrix} C_v & 0 & -D_v \\ 0 & I & 0 \end{bmatrix}, D = \begin{bmatrix} D_v \\ 0 \end{bmatrix}.$$

For control design purpose, we now define a cost function J as shown below :

$$J = E\{\int_{t_0}^{t_1} (e^T Q e + X_c^T R_c X_c + u_s^T R u_s) dt\} \quad (17)$$

where $E\{\}$ is the mathematical mean of statistical variable, Q and R_c are positive semi-definite matrices, and R is a positive definite matrix. Eq. (17) implies that three variables are to be constrained in the cost function, namely, the sensation error e along with the additional terms X_c and u_s, which together define the linear and angular motion of the platform. The cost function constrains both the sensation error and the platform motion.

Both the system equation and the cost function can be transformed to comply with the optimal control formulation as :

$$\dot{X} = A'X + Bu' + Hw$$
$$J' = E\{\int_{t_0}^{t_1} (X^T R_1' X + u'^T R_2 u') dt\} \quad (18)$$

where

$$A' = A - BR_2^{-1}R_{12}^T, u' = u_s + R_2^{-1}R_{12}^T X, R_1' = R_1 - R_{12}R_2^{-1}R_{12}^T,$$
$$R_1 = C^T G C, R_{12} = C^T G D, R_2 = R + D^T G D, G = diag[Q, R_c]$$

It is clear that the cost function of (18) is minimized when

$$u' = -R_2^{-1}B^T P X \quad (19)$$

where P is the solution of the algebraic Riccati equation

$$R_1' - PBR_2^{-1}B^T P + A'^T P + PA' = 0 \quad (20)$$

Substitute (19) into (18) to solve for u_s , then we get

$$u_s = -KX \quad (21)$$

where $K = R_2^{-1}(B^T P + R_{12}^T)$. Let K be partitioned according to the partition of X in (16), then we have :

$$u_s = -\begin{bmatrix} K_1 & K_2 & K_3 \end{bmatrix} \begin{bmatrix} X_e \\ X_c \\ X_n \end{bmatrix}. \quad (22)$$

Since $X_n = u_A$, we remove the state corresponding to X_n in Eq. (22) so that :

$$\begin{bmatrix} \dot{X}_e \\ \dot{X}_c \end{bmatrix} = \begin{bmatrix} A_v & 0 & -B_v \\ 0 & A_c & 0 \end{bmatrix} \begin{bmatrix} X_e \\ X_c \\ u_A \end{bmatrix} + \begin{bmatrix} B_v \\ B_c \end{bmatrix} u_s \quad (23)$$

Substitution of (22) into (23) then leads to

$$\begin{bmatrix} \dot{X}_e \\ \dot{X}_c \end{bmatrix} = \begin{bmatrix} A_v - B_v K_1 & -B_v K_2 \\ -B_c K_1 & A_c - B_c K_2 \end{bmatrix} \begin{bmatrix} X_e \\ X_c \end{bmatrix} + \begin{bmatrix} -B_v(I + K_3) \\ -B_c K_3 \end{bmatrix} u_A \quad (24)$$

After observing the state space forms respectively described by (24) and (13), the following equation can readily be derived in the Laplace domain:

$$u_s(s) = W(s) u_A(s) \quad (25)$$

with

$$W(s) = \begin{bmatrix} K_1 \\ K_2 \end{bmatrix}^T \begin{bmatrix} sI - A_v + B_v K_1 & B_v K_2 \\ B_c K_1 & sI - A_c + B_c K_2 \end{bmatrix}^{-1} \begin{bmatrix} B_v(I + K_3) \\ B_c K_3 \end{bmatrix} - K_3$$

being a matrix of the optimized transfer function which links the simulator inputs u_s to the vehicle inputs u_A.

4.2. Lateral Mode

For the lateral (roll/sway) mode, the algorithm under development is analogous to the longitudinal mode. In Eq. (1), the inputs $\dot{\theta}$ and a_x are replaced by $\dot{\phi}$ and a_y, respectively. The sensed rotational motion $\hat{\dot{\theta}}$ in Eq. (2) is now replaced by $\hat{\dot{\phi}}$, whereas the specific force f_x and sensed specific force $\hat{f}_x$ now become f_y and $\hat{f}_y$, respectively, all together satisfying

$$f_y = a_y - g\phi + r_{cp}\ddot{\phi}. \quad (26)$$

In turn, these changes lead to the different differential equation (cf. Eq. (9))

$$\begin{aligned} &\ddot{\hat{f}}_y + (b_0 + b_1)\dot{\hat{f}}_y + b_0 b_1 \hat{f}_y \\ &= G_{ot} K_{ot} (r_{cp}(b_0 + b_1 - a_0)\dot{\phi} \\ &+ (g + r_{cp} b_0 b_1)\phi + g a_0 \int \phi dt + \dot{a}_y + a_0 a_y) \end{aligned}$$

which, when being rewritten in a form similar to Eq. (10), will produce the state space representation for the otolith model similar to Eq. (11), with the same system matrices except that $D_{ot} = \begin{bmatrix} G_{ot} K_{ot} r_{cp} & 0 \end{bmatrix}$. To proceed further similarly, the state space representation for the vestibular model of the form of (13) will eventually be formulated. For this model, the additional platform states given in Eq. (14) are now $X_c = \begin{bmatrix} \iiint a_y dt^3 & \iint a_y dt^2 & \int a_y dt & \phi \end{bmatrix}^T$ instead.

The remaining derivation procedure is identical to that from Eqs. (15) to (25), resulting in a seventh-order transfer functions matrix $W(s)$ for the lateral mode.

4.3. Vertical Mode

For the vertical mode, or heave mode, the single degree-of-freedom input $u = a_z$, with the specific force $f_z = a_z - g$. The otolith model given in (5) then becomes

$$\hat{f}_z = \frac{G_{ot} K_{ot} (s + a_0)}{(s + b_0)(s + b_1)} f_z \quad (28)$$

and can then be defined in state space notation as

$$\begin{aligned} \dot{X}_{ot} &= A_{ot} X_{ot} + B_{ot} u \\ \hat{\dot{f}}_z &= C_{ot} X_{ot} + D_{ot} u \end{aligned} \quad (29)$$

where X_{ot} is the otolith state vector for this mode, and

$$A_{ot} = \begin{bmatrix} 0 & 1 \\ -b_0 b_1 & -(b_0 + b_1) \end{bmatrix}, B_{ot} = \begin{bmatrix} 0 \\ G_{ot} K_{ot} (a_0 - b_0 - b_1) \end{bmatrix},$$
$$C_{ot} = \begin{bmatrix} 1 & 0 \end{bmatrix}, D_{ot} = 0$$

Since this mode consists of a single translational degree-of-freedom, the formulation does not include the semicircular canals model, and therefore $A_v = A_{ot}$, $B_v = B_{ot}$, and $C_v = C_{ot}$. This results in a sensation model of the same form as (13):

$$\begin{aligned} \dot{X}_e &= A_v X_e + B_v u_s - B_v u_A \\ e &= C_v X_e \end{aligned} \quad (30)$$

Similar to the longitudinal mode, additional motion platform states are included in the state equations:

$$\dot{X}_c = A_c X_c + B_c u_s \quad (31)$$

where X_c represents the additional simulator states:

$$X_c = \begin{bmatrix} \iiint a_z dt^3 & \iint a_z dt^2 & \int a_z dt \end{bmatrix}^T,$$

and A_c and B_c now become

$$A_c = \begin{bmatrix} 0 & 1 & 0 \\ 0 & 0 & 1 \\ 0 & 0 & 0 \end{bmatrix}, B_c = \begin{bmatrix} 0 \\ 0 \\ 1 \end{bmatrix}$$

The vehicle input u_A now consists of a single channel of filtered white noise with break frequency γ, which can be expressed as

$$\begin{aligned} \dot{X}_n &= -\gamma X_n + \gamma w \\ u_A &= X_n \end{aligned} \quad (32)$$

The state equations given in (30), (31), and (32) can then be combined to form the desired system equation of the same form as (16), where y is the desired output, and $X = \begin{bmatrix} X_e & X_c & X_n \end{bmatrix}^T$ represents the integrated states. The remaining development procedure is identical to that from Eqs. (16) to (25), resulting in a single fourth-order transfer function for the vertical mode.

4.4. Yaw Mode

For the yaw mode, the single degree-of-freedom input is $u = \dot{\psi}$. The corresponding state space representation is the same as that in Eq. (4) with output $\dot{\psi}$ being replaced by $\hat{\dot{\theta}}$, namely,

$$\begin{aligned} \dot{X}_{sc} &= A_{sc} X_{sc} + B_{sc} u \\ \hat{\dot{\psi}} &= C_{sc} X_{sc} + D_{sc} u \end{aligned} \quad (33)$$

Since this mode consists of a single rotational input, the formulation does not include the otolith model, and therefore

we have $A_v = A_{sc}$, $B_v = B_{sc}$, $C_v = C_{sc}$, and $D_v = D_{sc}$. This results in a sensational model of the same form as (13):

$$\dot{X}_e = A_v X_e + B_v u_s - B_v u_A$$
$$e = C_v X_e + D_v u_s - D_v u_A \quad (34)$$

Similar to the longitudinal mode, additional motion platform states are included in the state equations as :

$$\dot{X}_c = A_c X_c + B_c u_s \quad (35)$$

where X_c represents the additional motion platform states, $X_c = \begin{bmatrix} \int \psi dt & \psi \end{bmatrix}$, and A_c and B_c now become

$$A_c = \begin{bmatrix} 0 & 1 \\ 0 & 0 \end{bmatrix}, B = \begin{bmatrix} 0 \\ 1 \end{bmatrix}$$

The vehicle input u_A now consists of a single channel of filtered white noise with break frequency γ, and can be expressed as

$$\dot{X}_n = -\gamma X_n + \gamma w$$
$$u_A = X_n \quad (36)$$

The state equations given in (34), (35), and (36) can then be combined to form the desired system equation of the same form as (16), where y is the desired output, and $X = \begin{bmatrix} X_e & X_c & X_n \end{bmatrix}^T$ represents the integrated states. The remaining development procedure is identical to that from Eqs. (16) to (25), resulting in a single fourth-order transfer function for the yaw mode.

5. EXPERIMENTAL RESULTS

In this section, we directly measure signals of the accelerations and rotational angles on body coordinate frame by a 3-axes accelerometer and a 2-axes tilt sensor respectively which attached on the Stewart platform to substitute for human vestibular system signals since the human vestibular system signals are not easy obtained. However, if measured signals (the accelerations and rotational angles) and command trajectories (the specific forces and angular velocity) is the same which mean that the Stewart platform motion achieve the same stimulation for human sensation. One experiment is done to compare HVB optimal washout filter algorithm with classical washout filter algorithm in performance and efficiency of platform's workspace in subsection 5.1.

5.1 Experimental of Surge Ramp Step and Roll Sinuous Testing

We used two degrees of freedom, the surge linear motion and roll angular motion, to test coordinated performances of our HVB washout filter and classical washout filter. The surge ramp step and roll sinuous motion for the experiment is as follows: 10s of a constant speed surge ($0 m/s^2$), after that 5s of a $0.2 m/s^3$ rate of increase in acceleration at 10s, then hold a constant acceleration at $1 m/s^2$ are adopted. In other hand, 30s of no turning of roll angular motion (0deg/s), after that we provide the sinuous roll motion with 10 deg/s magnitude and 1 rad/s^2 frequency are adopted.

The relative accelerometer measurements under surge (along *x* axis) and sway (along y axis) cases are plotted in Fig. 5 (a) and (b), respectively for comparison. After that the relative tilt sensor measurements under pitch and roll cases are plotted in Fig. 5 (c) and (d), respectively for comparison. Finally, the platform responsive trajectories of the every hydraulic leg by passing classical and HVB optimal washout filter are shown in Figs. 5 (e)-(j). Note all the black lines are the command inputs on the body coordinate frame. The red and blue lines are platform responsive trajectories by passing classical and HVB optimal washout filter, respectively. In this case, since some lengths of legs of the stewart platform are varied out of their mechanical limits, the classical washout filter algorithm could not repeat the testing trajectories. However, our scheme could still achieve testing trajectories. Hence, the HVB optimal washout filter approach was able to improve the efficiency of the platform workspace for running tasks.

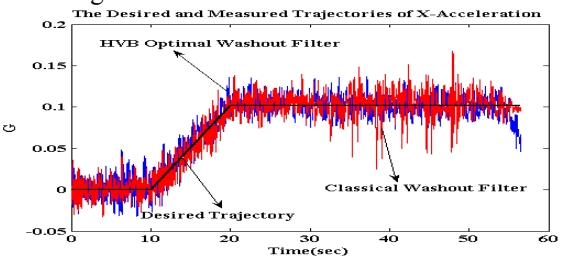

(a)

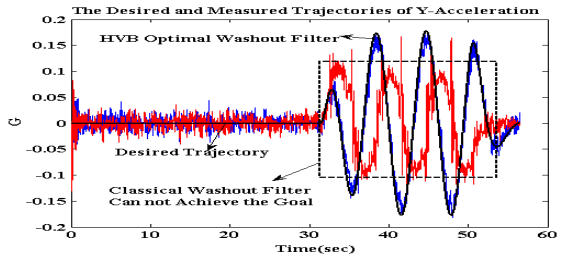

(b)

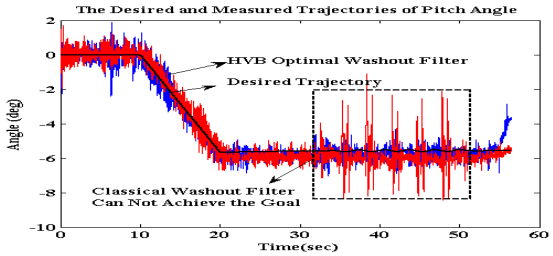

(c)

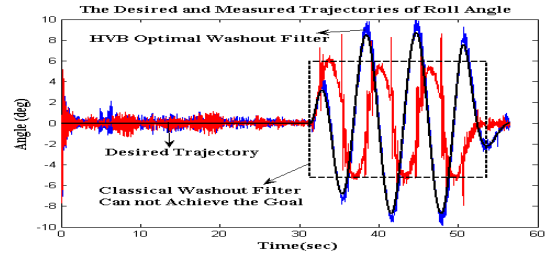

(d)

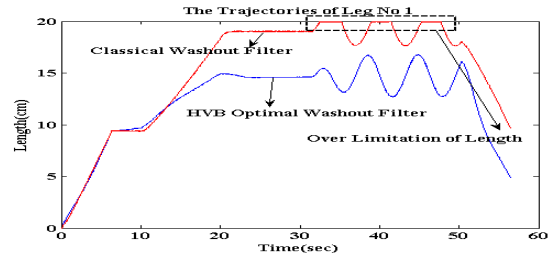

(e)

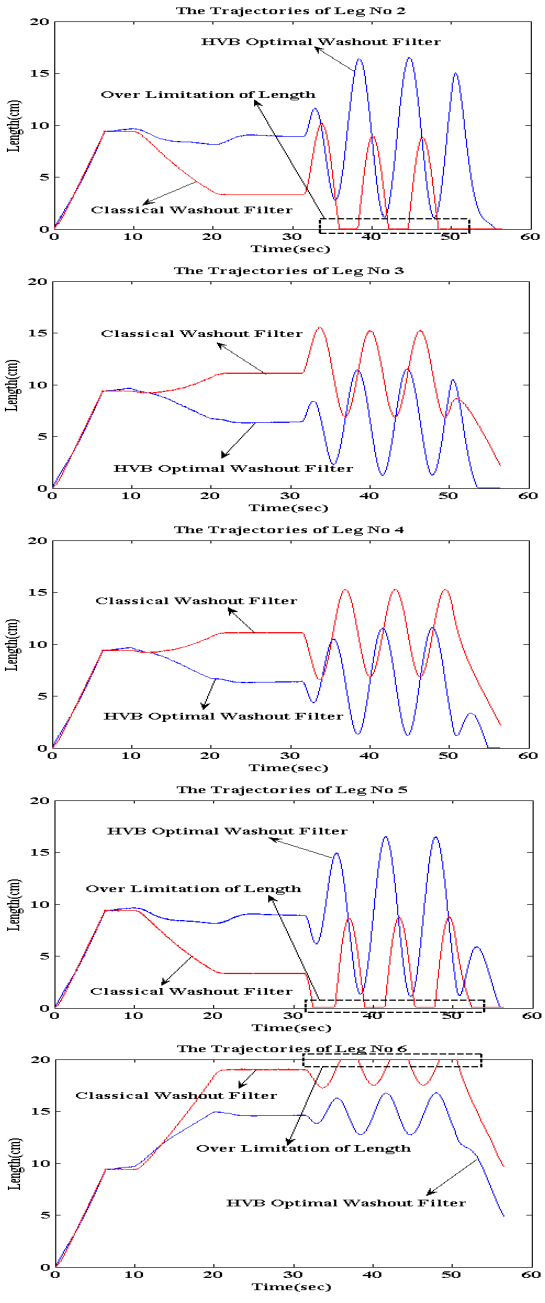

Fig. 5 The Stewart platform for tracking a surge ramp step and roll sinuous trajectory along x/y axis in the platform task space

6. CONCLUSIONS

In this paper, we have presented a new approach to developing washout filters for simulators. It is based on the human vestibular model, the senseless maneuver, and a motion platform limitation for designing a washout filter such that a cost function constraining the pilot's sensation error (between the simulator and vehicle) is minimized. The strong sensations experienced by the pilot can be curtailed, and the platform workspace for running tasks is more efficient. Finally, the simulation and experimental results confirm the effectiveness of our algorithm designed, and hence the advantages of the present approach can be manifested.

REFERENCES

[1] M.A. Nahon, L.D. Reid and J. Kirdeikis, "Adaptive Simulator Motion Software with Supervisory Control,", *Journal of Guidance, Control, and Dynamics*, vol.15, no.2 pp.376-383, 1992

[2] F. Barbagli, D. Ferrazzin, C.A. Avizzano and M. Bergamasco, "Washout Filter Design for a Motorcycle Simulator,", *IEEE International Conference on Systems, Man, and Cybernetics*, vol.2 pp.995-1000, 2000

[3] J.S. Yan and C.T. Lin, "Auto-tuning Washout Filter and its Application to VR- based Ship Dynamic Simulation System" Master Thesis of NCTU 2001

[4] M. Idan and M.A. Nahon, "Off-Line Comparison of Classical and Robust Flight Simulator Motion Control,", *Journal of Guidance, Control, and Dynamics*, vol.22, no.5 1999

[5] M.K. Park, M.C Lee, K.S. Yoo, K. Son, W.S. Yoo, and M.C. Han, "Development of the PNU Vehicle Driving Simulator and Its Performance Evaluation,", *Proceeding of IEEE International Conference on Robotics and Automation*, pp.2325-2330 2001

[6] M.A. Nahon and L.D. Reid, "Simulator Motion- Drive Algorithm: A Designer's Perspective," *Journal of Guidance, Control, and Dynamics*, vol.13, no.2 pp.356- 362,1990

[7] Website: www.medicine.mcgilli.ca

[8] M. Idan and D. Sahar, "A Robust Controller for a Dynamic Six Degree of Freedom Flight Simulator," *AIAA Proc. Of conf. on Flight Simulator Technologies*, pp. 53-60, 1996

[9] R. Sivan, J. Ish -Shalom .and J. K. Huang, "An Optimal Control Approach to the Design of Moving Flight Simulations," *IEEE Transactions on Systems, Man and Cybernetics*, vol. 12, no. 6, pp. 818-827, 1982.

[10] D. Ariel and R. Sivan, "False Cue Reduction in Moving Flight Simulators," *IEEE Transactions on Systems, Man and Cybernetics*, vol. 14, no. 4, pp. 665-671, 1984.

Table 3 Human Vestibular Model Parameter [5]

Parameter	Pitch/Surge	Roll/Sway	Yaw/Heave
Semicircular Canals $\dot{\hat{\theta}} = \frac{G_{sc}\tau_1\tau_a s^2(1+\tau_L s)}{(1+\tau_a s)(1+\tau_1 s)(1+\tau_2 s)}\dot{\theta}$			
τ_1(sec)	5.73	5.73	5.73
τ_2(sec)	0.005	0.005	0.005
τ_a(sec)	80	80	80
τ_L(sec)	0.06	0.06	0.06
G_{scc} Threshold Units	28.6479	28.6479	0.06
Threshold(deg/s)	2.0	2.0	1.6
Otolith $\hat{f}_z = \frac{G_{ot}K_{ot}(s+a_0)}{(s+b_0)(s+b_1)}f_z$			
a_0(sec^{-1})	0.1	0.1	0.1
b_0(sec^{-1})	0.2	0.2	0.2
b_1(sec^{-1})	62.5	62.5	
G_{ot} Threshold(m/s2)	4.7059 *b1	4.7059*b1	2.8571
Threshold(m/s2)	0.17	0.17	0.28